Am J Transl Res 2017;9(2):330-342
www.ajtr.org /ISSN:1943-8141/AJTR0039993

Original Article

Receptor for advanced glycation end as drug targets in diabetes-induced skin lesion

Xiang-Fang Chen[1*], Wei Tang[1*], Wei-Dong Lin[2], Zi-Yu Liu[1], Xiao-Xiao Lu[1], Bei Zhang[1], Fei Ye[1], Zhi-Min Liu[1], Jun-Jie Zou[1], Wan-Qing Liao[3]

Departments of [1]Endocrinology, [3]Dermatology, Changzheng Hospital, Second Military Medical University, Shanghai 200003, China; [2]Department of Burns, Shanghai Fire Corps Hospital Chinese People's Armed Police, Shanghai 200443, China. [*]Equal contributors.

Received August 18, 2016; Accepted January 17, 2017; Epub February 15, 2017; Published February 28, 2017

Abstract: The involvement of the receptor for advanced glycation end (RAGE) in different diseases has been reviewed in great detail, previously, but the effects of diabetic drugs on RAGE-induced skin lesion during long course diabetes remains poorly understood. In the present study, we have shown that RAGE was overexpressed in both diabetic rats and human keratinocytes (HaCaT cells). Cell cycle arrest and apoptosis as well as alternations of relative protein levels were also found in diabetic rats and HaCaT cells with overexpression of RAGE that were rectified by metformin (Met) treatment. Moreover, overexpression of RAGE was also found to induce secretions of TNF-α, IL-1β, IL-6, ICAM-1 and COX-2 in HaCaT cells, and Met treatment corrected these inflammatory factor secretions. In addition, treatment with Met markedly reduced RAGE overexpression-induced p38 and NF-κB activation. Taken together, the findings of the present study have demonstrated, for the first time that Met protects HaCaT cells against diabetes-induced injuries and inflammatory responses through inhibiting activated RAGE.

Keywords: Diabetes, RAGE, apoptosis, inflammatory response, drug target

Introduction

Diabetes is a common epidemic disease characterized by insulin resistance, hyperglycemia, and dysfunctions in metabolism of lipids and carbohydrates [1]. Worldwide, diabetes is estimated to have affected 382 million people in 2013, with a projected increase to 657 million cases by 2035 [2]. The complications associated with diabetes are a major cause of mortality. Skin lesions are a serve and frequent complication of diabetes caused by neuropathy and ischemia, and are oftenone of the first presenting signs of diabetes.

Advanced glycosylation productions (AGEs) accumulation on skin collagen is found during the normal process of aging, in diabetes or chronic renal failure interfering normal skin function [3]. The receptor for AGE (RAGE) is expressed in a variety of tissues and cells and plays an important role in AGEs-activated signaling mechanisms associated with cell stress, cellular dysfunction, and can lead to other complications. Experiments in animal models of diabetes revealed that blockade of RAGE suppressed accelerated atherosclerosis and resulted in attenuation of functional and pathological endpoints of nephropathy in diabetic mouse models [4, 5]. Given the roles played by RAGE in inflammatory mechanisms, experiments have been performed to demonstrate the effects of RAGE stimulation on two key transcription factors, NF-κB and early growth response-1 [6, 7]. It is well established that RAGE ligation by AGE stimulates signal transduction cascades such as mitogen-activated protein kinases (MAPK), phosphatidylinositol 3-kinase (PI3K), Janus kinase/signal transducers and activators of transcription (JAK/STAT), thus leading to the activation of nuclear transcription factors, such as NF-κB and c-myc [8]. However, the role of RAGE in diabetes-induced skin lesions has remained largely unclear.

Metformin (Met) is used as an insulin sensitizer that can reduce cardiovascular morbidity and mortality as well as the incidence of several

non-communicable diseases in diabetic subjects. Previous studies have shown that Met inhibited proliferation and proinflammatory responses in HaCaT cells by inhibition of the mTOR [9] and ERK1/2 signaling pathways [10]. Met may have therapeutic potential in diabetic nephropathy by blocking the AGEs-RAGE-ROS axis through AMP-activated protein kinase activation [11, 12]. Moreover, Met treatment has been shown to reduce cell proliferation and improve wound healing in an animal model and affects clinical outcomes in diabetic foot ulcer patients [13].

In the present study, the effects of Met on keratinocytes cell cycle, apoptosis and inflammation, and the regulatory protein expression were evaluated and the molecular mechanisms of action of Met in the treatment of diabetes were investigated.

Material and methods

Patients

Ulcer skin tissues and peripheral blood samples of 60 patients with diabetic ulcer (30 1-2 diabetic ulcer severity score [DUSS] and 30 3-4 DUSS); 40 females and 20 males, mean age 64±13 years) and 30 healthy individuals (21 female and 9 male, mean age 52±12 years) in Changzheng Hospital, were recruited for real-time PCR and enzyme linked immunosorbent assay. All individuals involved in this study gave informed consent. The study was approved by the regional ethics committee in Changzheng Hospital.

Experimental animals and treatment

Eighteen specific-pathogen-free male Sprague-Dawley (SD) rats (age, 8 weeks; weight, 200-220 g) were purchased from the Shanghai Laboratory Animal Center of Chinese Academy of Medical Sciences. Care of the laboratory animals and animal experiments were performed in accordance with animal ethics guidelines and approved protocols. The 18 SD rats were randomized into three groups: an untreated control group (six rats), a diabetic rat group (six rats) and a Met treatment group (six rats). Rats in the diabetic group received 65 mg/kg of STZ citrate buffer intraperitoneally to induce diabetes. Rats were categorized as diabetic when their blood glucose exceeded 16.7 mM at 48 h after first STZ injection. Rats in the Met treatment group were given a single intraperitoneal injection containing 100 mg/kg Met in citrate buffer 72 h after STZ injection. Twelve weeks after the diabetic induction, all rats were killed for analysis. Epidermal keratinocytes were acquired from rat skin samples as previously described [14], cultured in serum-free skin cell culture medium (K-SFM) (Gibco, Rockville, MD, USA) for two weeks, and changes in the levels of cell cycle and apoptosis-related factors were determined by real-time PCR and Western blot analysis.

Cell culture

Human keratinocytes HaCaT cells were obtained from Cobioer Biosciences Co., Ltd (Nanjing, China) cultured in Dulbecco's modified Eagle's medium (DMEM, Hyclone, Logan, Utah, USA) with 10% fetal bovine serum (Gibco), penicillin (100 U/ml, Solarbio, Beijing, China) and streptomycin (100 μg/ml, Solarbio) supplemented. Primary epidermal keratinocytes were seeded in a 6-wellplate containing 4 ml of serum-free K-SFM (Hyclone). Both HaCaT cells and epidermal keratinocytes were incubated in a humidified atmosphere at 37°C with 5% CO_2.

Vector construction

pLV-IRES-eGFP, VSV-G and pol/gag were purchased from Addgene (Cambridge, MA, USA). Plasmid containing full-length RAGE was purchased from Sangon Biotech Co., Ltd (Shanghai, China). The full-length RAGE was amplified using PCR. The primers used were as follows: RAGE-forward, 5'-CGGAATTCCATGGACCTGTGGAGC-3' and RAGE-reverse, 5'-CGCGGATCCGTTATCTTCCGCCTTT-3'. The PCR products were then digested using *Eco*R I and *Bam*H I and cloned into pLV-IRES-eGFP.

Lentiviral production and transduction

RAGE was delivered into HaCaT cells by using alentiviral transfection system. Briefly, 239T cells were seeded in a 6-well plate and after 24 h were co-transfected with 2 μg of plasmid vector, 1 μg pLV-IRES-eGFP-RAGE, 0.1 μg VSV-G, and 0.9 μg pol/gag by using Lipofectamine 2000 (Thermo Fisher Scientific Inc., Rockford, IL, USA) according to the manufacturer's instructions. The recombinant lentivirus pLV-IRES-eGFP-RAGE was collected 48 h after

transfection and used to infect HaCaT cells. The blank pLV-IRES-eGFP was used as the negative control.

Cell viability assay

HaCaT cell viability was evaluated by 3-(4,5-dimethylthiazol-2-yl)-2,5-diphenyltetrazolium bromide (MTT) assay as previously described [15]. In brief, the cells were seeded in 96-well culture plates and infected with or without pLV-IRES-eGFP-RAGE in the absence or presence of Met (100 μM) for 12, 24, 48, and 72 h. Subsequently, cell viability was evaluated by MTT assay. The absorbance was measured at a 490 nm test wavelength and 570 nm reference wavelength with a spectrophotometric microplate reader (Bio-Tek, Winchester, USA).

Cell cycle and apoptosis assay

HaCaT cells were seeded in 6-well culture plates and infected with or without pLV-IRES-eGFP-RAGE in the absence or presence of Met (100 μM) for 48 h. For cell cycle assay, the cells were harvested, washed with PBS, fixed with 75% ethanol at -20°C for 24 h and treated with 1 mg/ml RNase A (Sigma, Sydney, Australia) at 37°C for 1 h. After washing, the cells were stained with 50 μg/ml propidium iodide (PI, Beyotime Biotechnology, Shanghai, China) in the dark at room temperature for 10 min. For cell apoptosis assay, cells were harvested, washed with PBS, resuspended with 195 μl of annexin-V FITC (BD Biosciences, Franklin Lakes, NJ, USA) and 5 μl of PI following the manufacturer's protocol and then incubated for 10 min in the dark at room temperature. Analysis was performed by flow cytometry and analyzed using Lysis software (EPICS-XL, Ramsey, Minnesota, USA).

Mitochondrial membrane potential (Δψm) and intracellular reactive oxygen species (ROS) analysis

HaCaT cells were seeded in 6-well culture plates and infected without or with pLV-IRES-eGFP-RAGE in the absence or presence of Met (100 μM) for 48 h. For Δψm assay, the cells were harvested, washed with PBS, incubated with 100 nM TMRE (Immuno Chemistry Technologies, LLC, Bloomington, MN, USA) for 20 min at 37°C in the dark and then subjected to flow cytometry analysis. For ROS assay, the cells were harvested, washed with PBS, incubated with 50 μM DHE (Vigorous Biotechnology, Beijing, China) following the manufacturer's protocol, and fluorescence intensity was measured using flow cytometry.

Enzyme linked immunosorbent assay

HaCaT cells were seeded in 6-well culture plates and infected without or with pLV-IRES-eGFP-RAGE in the absence or presence of Met (100 μM) for 48 h. The relative concentration of each secreted inflammatory factor in the supernatant was measured by enzyme-linked immunosorbent assay (ELISA) according to the manufacturer's protocol.

RT-PCR and real-time PCR

Total RNA was extracted using TRIzol reagent (Thermo Fisher Scientific Inc.), according to the manufacturer's instructions. The cDNA was synthesized using a cDNA synthesis kit (Thermo Fisher Scientific Inc.). Real-time RT-PCR assay was performed using SYBR Green (Takara Biotechnology Co., Ltd, Dalian, China), and data collection was conducted using an ABI 7300 (Applied Biosystems, Foster City, CA, USA). Sequences for the primers are as follows: RAGE-forward: 5'-CGGCTGGAATGGAAACTG-3' and RAGE-reverse: 5'-TAGACACGGACTCGGTAG-3'; GAPDH-forward: 5'-CACCCACTCCTCCACCTT-TG-3' and GAPDH-reverse: 5'-CCACCACCCTGT-TGCTGTAG-3'. GAPDH was used as an internal control for normalization. The gene expression was calculated using the $2^{-\Delta\Delta Ct}$ method.

Western blot

Cells were seeded at a density of 1×10^5 cells per well in 6-well plates, cultured overnight, and then infected without or with pLV-IRES-eGFP-RAGE in the absence or presence of Met (100 μM) for 6 h or 48 h. Cells were harvested and lysed on ice for 30 min in RIPA buffer (Beyotime) containing 1 mM phenylmethylsulfonyl fluoride (PMSF). 30 μg proteins were separated on 12% SDS-PAGE gels and transferred onto a polyvinylidenedifluoride (PVDF) membrane. Then the blots were incubated with primary antibodies specific to p21 (1:500, Abcam, Cambridge, MA, USA), Gadd45a (1:500, Abcam), CyclinB1 (1:1000, Abcam), CyclinD1 (1:2000, Cell Signaling Technology [CST], Inc., Beverley, MA, USA), CDK4 (1:2000, CST), p-p53

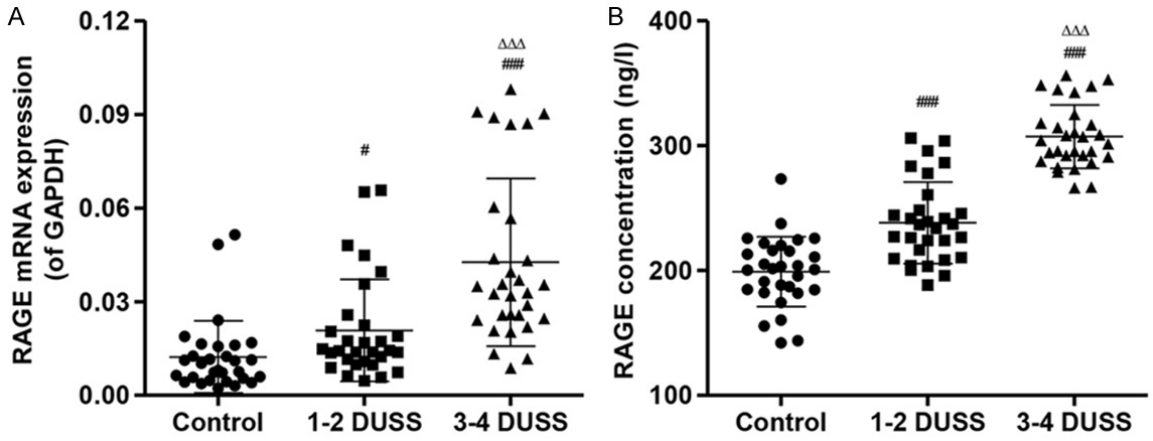

Figure 1. RAGE levels in ulcerous skin tissues and peripheral blood of diabetic patients. The RAGE levels in ulcerous skin tissues and peripheral blood of diabetic patients were measured by real-time PCR (A) and Elisa assay (B), respectively. $^{\#}P<0.05$, $^{\#\#\#}P<0.001$ vs. Control. $^{\Delta\Delta\Delta}P<0.001$ vs. 1-2 DUSS.

Table 1. Clinical features of patients with diabetic ulcer

	1-2 DUSS	3-4 DUSS	*P* value
Gender (female/male)	18/12	22/8	0.184
Age (years), median	63 (51-79)	61 (45-71)	0.087
Time with ulcerative process (days), median	127 (68-219)	148 (97-250)	0.254
Time of hospitalization (days), median	4 (3-7)	5 (4-7)	0.351
BMI (kg/m^2), median	26.8 (21.4-28.1)	25.9 (22.5-27.1)	0.417
Ischemia (yes/no)	20/10	23/7	0.987
Infection (yes/no)	19/11	28/2	0.034*
Glucose (mg/dL), median	224.3 (152.1-289.2)	201.9 (138.1-378.4)	0.893
Hemoglobin (g/dL), median	10.8 (9.4-11.6)	11.2 (9.1-13.1)	0.627
WBC	11.8 (9.6-13.1)	12.9 (9.9-11.2)	0.487

BMI: Body mass index; WBC: white blood cell; *, $P<0.05$, calculated by Fisher's exact test.

(1:1000, Abcam), p53 (1:1000, Abcam), caspase-3 (1:1000, CST), Bax (1:200, Santa Cruz Biotechnology, Inc., Santa Cruz, CA, USA), Bcl-2 (1:200, Santa Cruz), p-p38 (1:1000, CST), p38 (1:1000, CST), p-NF-κBp65 (1:1000, CST), NF-κBp65 (1:1000, CST), TNF-α (1:5000, Abcam), IL-1β (1:500, Santa Cruz), IL-6 (1:100, Abcam), ICAM-1 (1:200, Abcam), COX-2 (1:500, Abcam), and GAPDH (1:1500, CST) overnight with gentle agitation at 4°C, followed by incubation with horseradish peroxidase-conjugated secondary antibodies (1:1000, Beyotime) for 1 h at 37°C. The blots were visualized using enhanced chemiluminescence (Millipore, Billerica, MA, USA) and signals were quantified by Image J 1.41 software (National Institute of Health, Bethesda, MD, USA).

Statistical analysis

All data were expressed as the mean ± SD and were representative of experiments done in triplicate. Statistical analyses were performed using SPSS 19.0 (IBM Corporation, Armonk, NY, USA). Unpaired two-tailed t test and one-way ANOVA analyses were used to compare the data from different groups. $P<0.05$ was considered significant.

Results

RAGE levels in ulcer skin tissues and peripheral blood of patients with diabetes

In order to study the role of RAGE in diabetes, we first measured the levels of RAGE in ulcer-

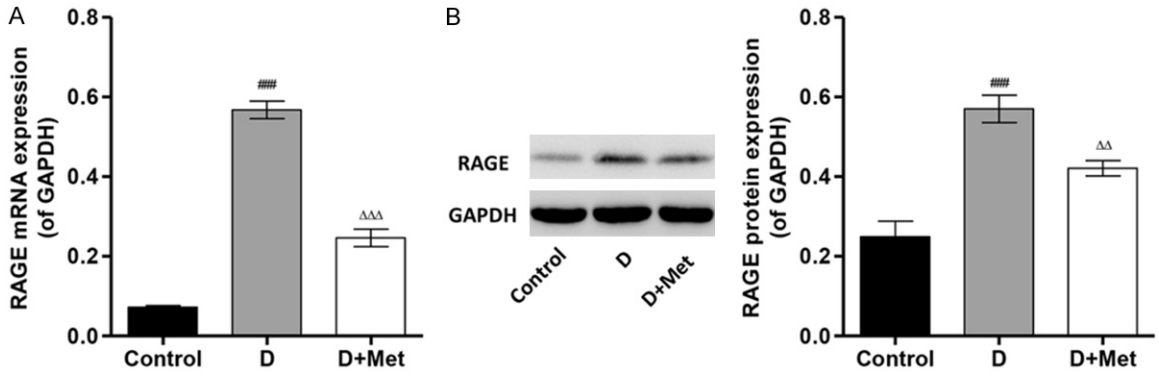

Figure 2. Effect of Met treatment on RAGE expression in diabetic rats. After intraperitoneal injection with STZ (n=6) for 72 h, rats were treated with Met at 100 μM for 48 h. Expression of RAGE was measured by real-time PCR (A) and western blot (B). $^{###}P<0.001$ vs. Control. $^{ΔΔΔ}P<0.001$ vs. Diabetes.

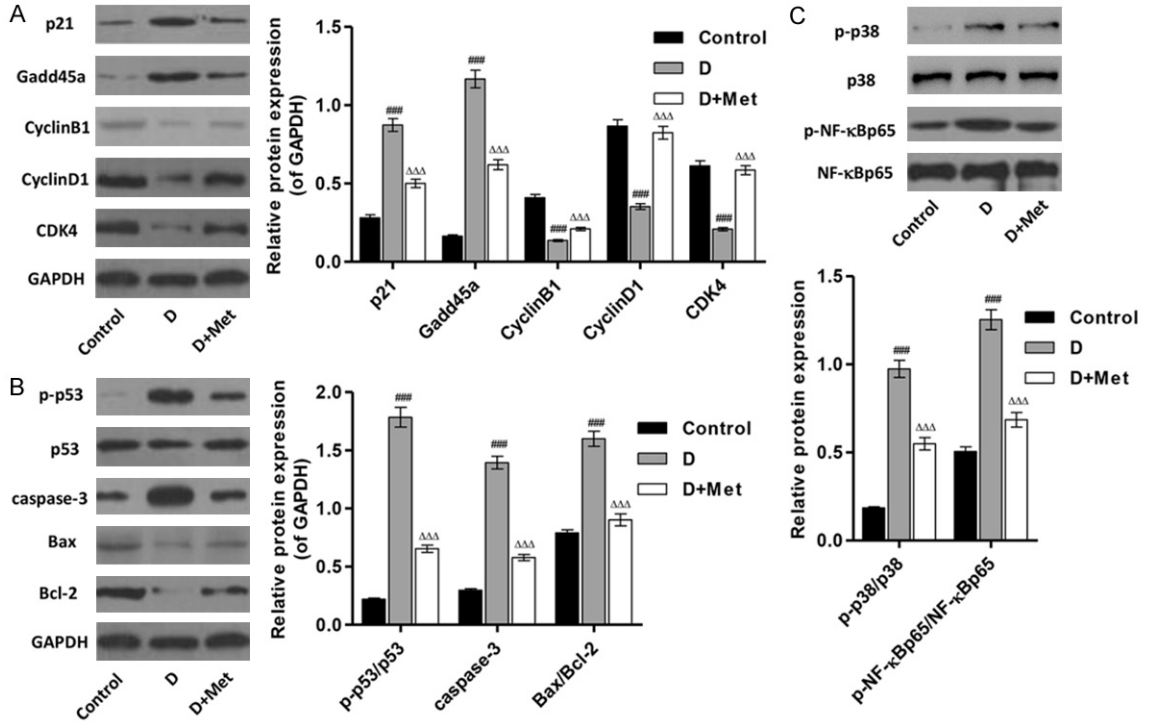

Figure 3. Effect of Met treatment on cell cycle and apoptosis in diabetic rats. After intraperitoneal injection with STZ (n=6) for 72 h, rats were treated with Met at 100 μM. Expression of cell cycle-related protein (A), including p21, Gadd45a, CyclinB1, CyclinD1, and CDK4, cell apoptosis-related protein (B, C), including p-p53, p53, caspase-3, Bax and Bcl-2, p-p38, p38, p-NF-κBP65, and NF-κBP65 was measured by western blot. $^{###}P<0.001$ vs. Control. $^{ΔΔΔ}P<0.001$ vs. Diabetes.

ous skin tissues and peripheral blood of patients with diabetes (n=60) alongside healthy controls (n=30). As shown in **Figure 1A** and **1B**, RAGE expressions in ulcer skin tissues and peripheral blood were significantly increased in patients with diabetes when compared to healthy control samples. Importantly, higher levels of RAGE were observed in samples from patients with higher diabetic ulcer severity scores (3-4 DUSS) than that with lower scores (1-2 DUSS). These results suggested that RAGE might play an important role in the progression of diabetic skin lesions, and RAGE was therefore used for subsequent experiments.

Given that this observation might have important clinical repercussions for patients that have chronic wounds such as diabetic ulcer, we

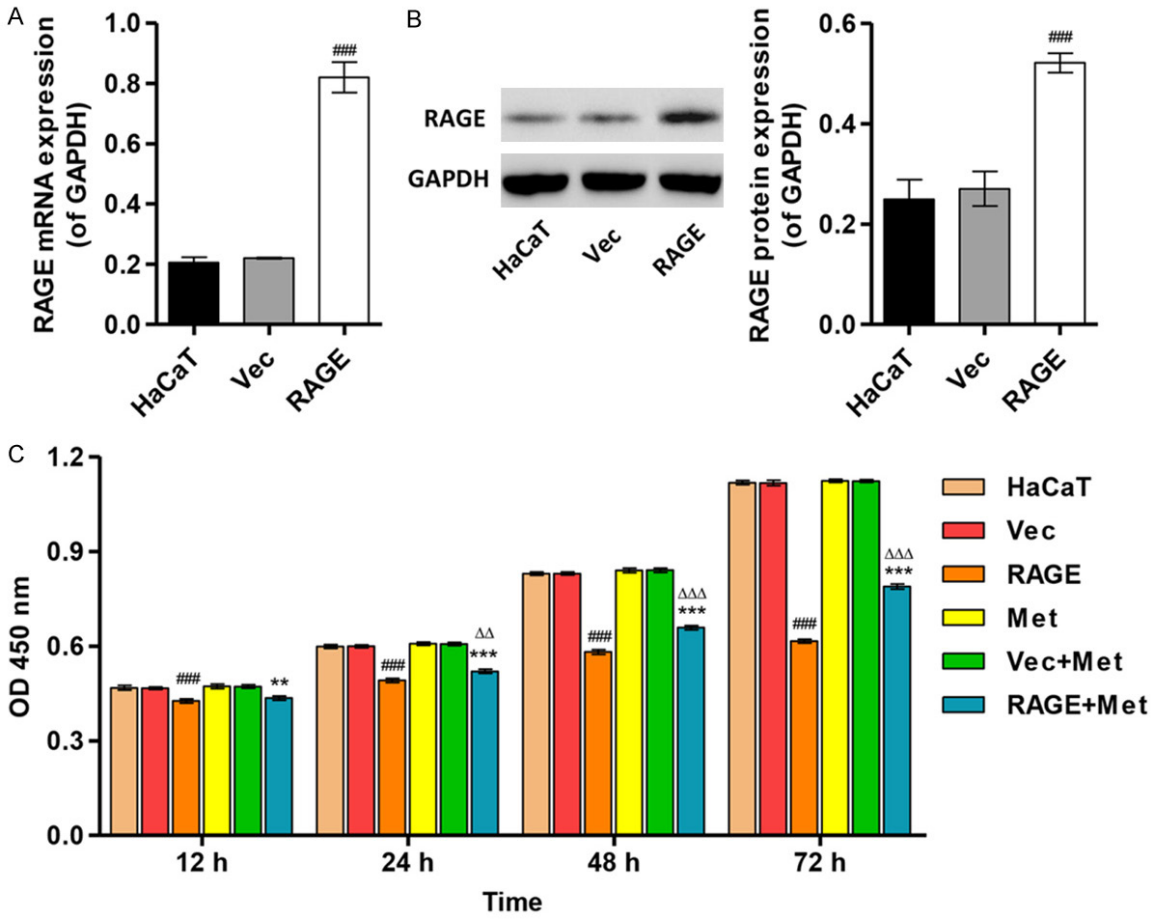

Figure 4. Met protects HaCaT cells against RAGE overexpression-induced cytotoxicity. HaCaT cells were infected with pLV-IRES-eGFP-RAGE for 48 h, and the expression of RAGE was measured by real-time PCR (A) and western blot (B). After infected with pLV-IRES-eGFP-RAGE for 48 h, HaCaT cells were treated with Met at 100 μM for 12, 24, 48 and 72 h (C). Cell viability was measured by MTT assay. $^{###}P<0.001$ vs. Vec. $^{**}P<0.01$, $^{***}P<0.001$ vs. Vec+Met. $^{\Delta\Delta}P<0.01$, $^{\Delta\Delta\Delta}P<0.001$ vs. RAGE.

analyzed a group of patients from the Changzheng Hospital who were admitted for chronic ulcers, and who had more complete information in their clinical file. Sixty cases were selected for this analysis. From these files, the patients were stratified according to the treatment they were receiving at the time of admission to the hospital. The general characteristics of these patients are described in **Table 1**. Statistically significant differences were found after stratification for the proportion of subjects with infection. For all the other variables analyzed, no differences were found.

Met inhibits RAGE overexpression in STZ-induced diabetic rats

To investigate the effect of RAGE expression on diabetic rats *in vivo*, real-time PCR and western blot analyses were performed. As shown in **Figure 2A** and **2B**, diabetic rats (induced by intraperitoneal injection with STZ) showed an overexpression of RAGE at both mRNA (0.57±0.02 vs. 0.07±0.01, n=6) and protein levels (0.57±0.03 vs. 0.25±0.04, n=6). However, the RAGE overexpression induced by diabetes was significantly inhibited by Met treatment with 100 mg/kg for 48 h (mRNA level, 0.25±0.02 vs. 0.57±0.02, n=6; protein level, 0.42±0.02 vs. 0.57±0.03, n=6). These results indicate that Met inhibits STZ-induced RAGE overexpression in diabetic rats.

Met suppresses cell cycle arrest and cell apoptosis in STZ-induced diabetic rats

To elucidate whether the protection of Met was associated with its inhibition of cell cycle arrest

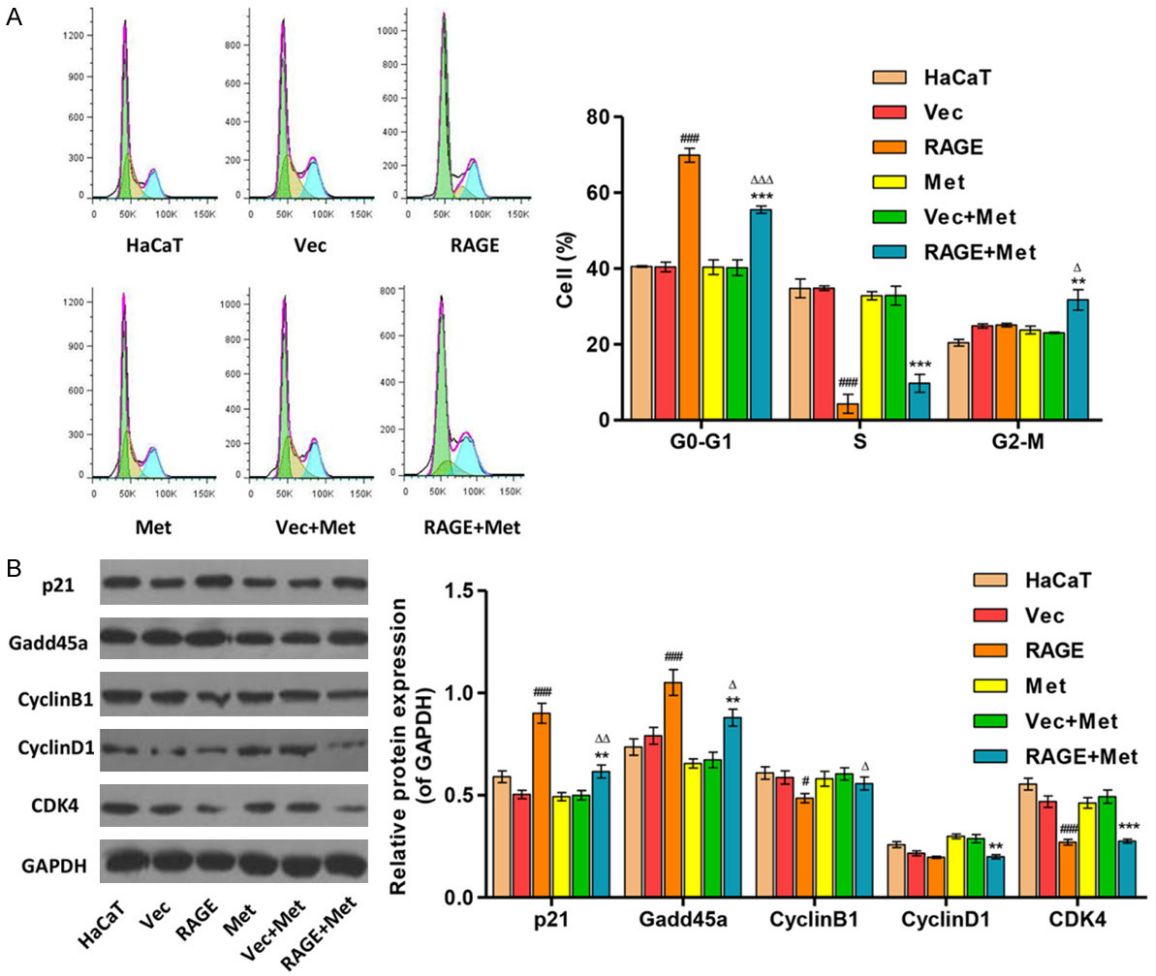

Figure 5. Met protects HaCaT cells against RAGE overexpression-induced cell cycle arrest. After infected with pLV-IRES-eGFP-RAGE for 48 h, HaCaT cells were treated with Met at 100 μM for 48 h. Cell cycles were measured by PI staining and flow cytometry (A). Expression of cell cycle-related proteins, including p21, Gadd45a, CyclinB1, CyclinD1, and CDK4, was measured by Western blot (B). $^{\#}P<0.05$, $^{\#\#\#}P<0.001$ vs. Vec. $^{**}P<0.01$, $^{***}P<0.001$ vs. Vec+Met. $^{\Delta}P<0.05$, $^{\Delta\Delta}P<0.01$, $^{\Delta\Delta\Delta}P<0.001$ vs. RAGE.

in STZ-induced diabetic rats, cell cycle-related protein levels were measured by western blot analysis. Intraperitoneal injection of rats with STZ led to an upregulation of p21 and Gadd45a protein levels, while also resulting in a down-regulation of CyclinB1, CyclinD1 and CDK4 protein levels (**Figure 3A**). However, the alterations of these protein levels induced by diabetes were significantly corrected by Met treatment with 100 mg/kg for 48 h.

Next, we measured apoptosis in response to diabetes and Met. As shown in **Figure 3B**, increased caspase-3 expression and increased ratio of p-p53/p-53 and Bax/Bcl-2 were also found in diabetic rats. These were significantly corrected by Met treatment with 100 mg/kg. Moreover, intraperitoneal injection of rats with STZ significantly enhanced intranuclear p-p38 and NF-κBp65 subunit expression, and the central status of p38 and NF-κB activation, respectively (**Figure 3C**). However, treatment of Met with 100 mg/kg significantly inhibited p-p38 and NF-κBp65 subunit nuclear translocation. These results suggest that the protection of Met against cell cycle arrest and apoptosis caused by diabetes is partially associated with the regulation of these molecules and signaling pathways *in vivo*.

Met represses RAGE overexpression-induced cytotoxicity in HaCaT cells

To investigate the effect of Met on RAGE overexpression-induced cytotoxicity in HaCaT cells

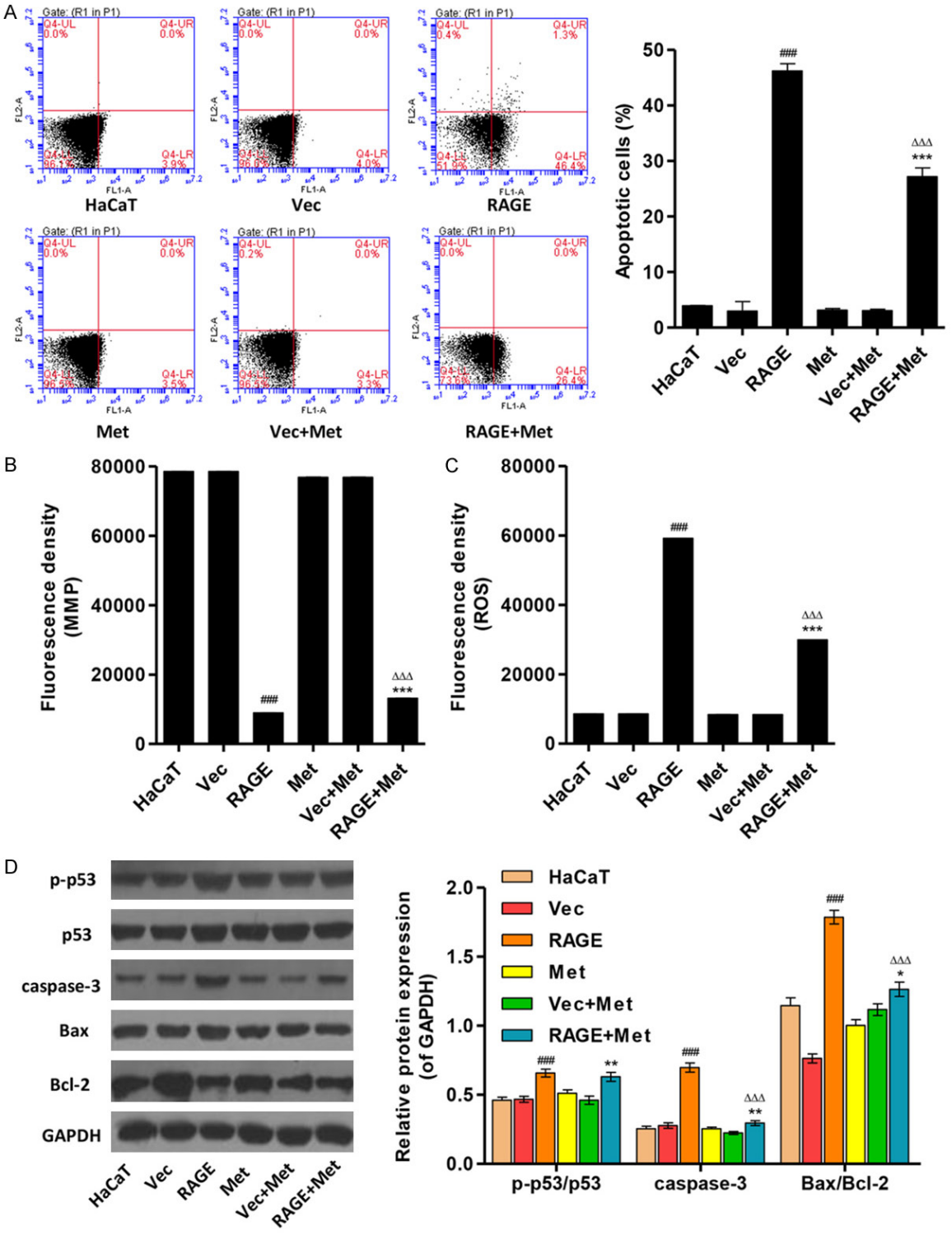

Figure 6. Met protects HaCaT cells against RAGE overexpression-induced cell apoptosis. After infected with pLV-IRES-eGFP-RAGE for 48 h, HaCaT cells were treated with Met at 100 μM for 48 h. Cell apoptosis was measured by annexin-V FITC and PI staining and flow cytometry analysis (A). Changes of Δψm (B) and ROS production (C) in HaCaT cells were measured by flow cytometry analysis, respectively. Expression of cell apoptosis-related proteins, including p-p53, p53, caspase-3, Bax, and Bcl-2, was measured by western blot (D). $^{###}P<0.001$ vs. Vec. $^{*}P<0.05$, $^{**}P<0.01$, $^{***}P<0.001$ vs. Vec+Met. $^{ΔΔΔ}P<0.001$ vs. RAGE.

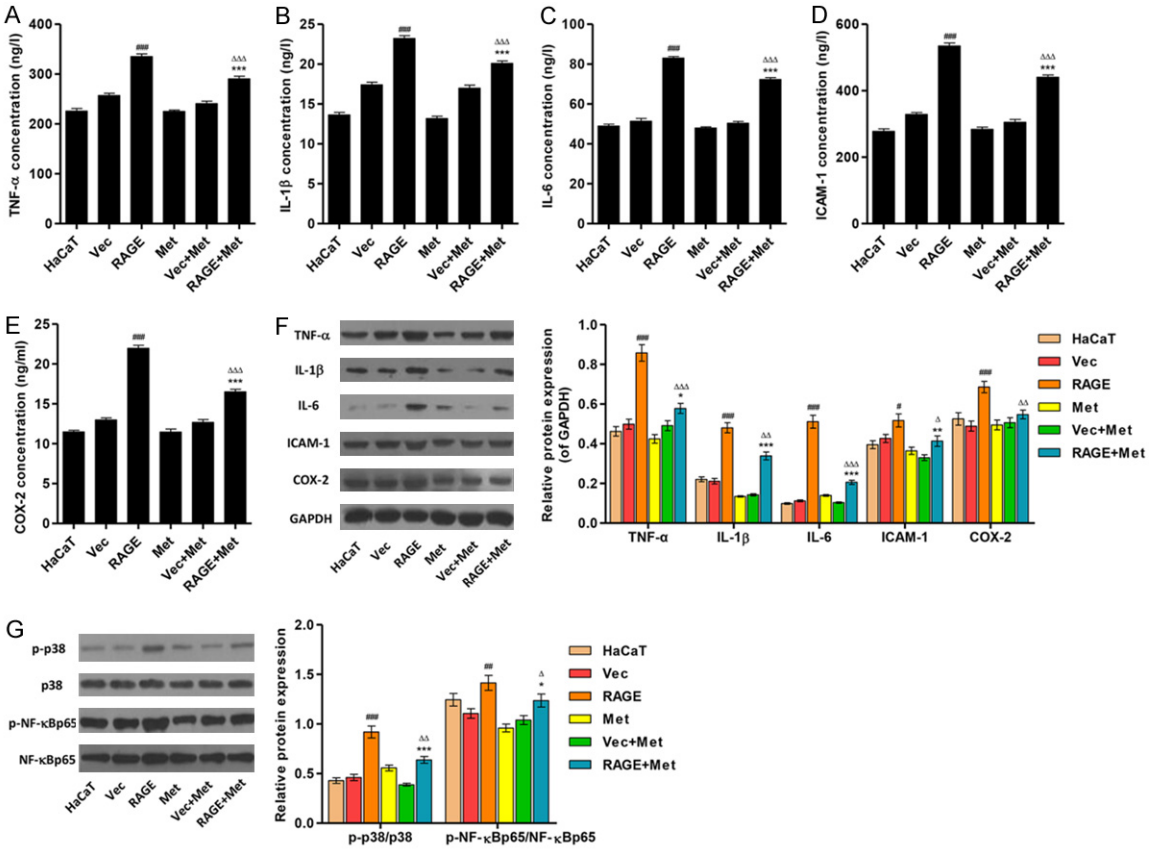

Figure 7. Met protects HaCaT cells against RAGE overexpression-induced inflammatory responses and activation of p38/NF-κB. After infected with pLV-IRES-eGFP-RAGE for 48 h, HaCaT cells were treated with Met at 100 μM for 48 h. The levels of TNF-α (A), IL-1β (B), IL-6 (C), ICAM-1 (D) and COX-2 (E) in HaCaT cells were measured by ELISA and western blot (F). Expression of p-p38, p38, p-NF-κBP65, and NF-κBP65 was measured by western blot (G). $^{\#}P<0.05$, $^{\#\#}P<0.01$, $^{\#\#\#}P<0.001$ vs. Vec. $^{*}P<0.05$, $^{**}P<0.01$, $^{***}P<0.001$ vs. Vec+Met. $^{\Delta}P<0.05$, $^{\Delta\Delta}P<0.01$, $^{\Delta\Delta\Delta}P<0.001$ vs. RAGE.

in vitro, HaCaT cells with RAGE stable expression was constructed by infection with pLV-IRES-eGFP-RAGE, and cell viability was detected by MTT assay. As shown in **Figure 4A** and **4B**, RAGE expressions in HaCaT cells were increased significantly in mRNA (0.82±0.05 vs. 0.22±0.02) and protein levels (0.52±0.02 vs. 0.27±0.03). RAGE overexpression in HaCaT cells led to a decrease in cell viability in a time-dependent manner compared with HaCaT cells with blank vector infection (**Figure 4C**). However, the decreased cell viability induced by RAGE overexpression in HaCaT cells was significantly inhibited by treatment with Met at 100 μM in a time-dependent manner. These findings demonstrate that Met treatment protects against RAGE overexpression-induced toxicity in HaCaT cells.

Met represses RAGE overexpression-induced cell cycle arrest in HaCaT cells

To elucidate whether the cytoprotection of Met was associated with its inhibition of cell cycle arrest in RAGE overexpression-induced HaCaT cells, cell cycle assay was measured by PI staining and flow cytometry. RAGE overexpression in HaCaT cells led to an increased number of G0-G1 phase cells (69.87±1.83% vs. 40.43±1.25%) and a decreased number of S phase cells (4.33±2.45% vs. 34.84±0.60%) compared with HaCaT cells with blank vector infection, suggesting RAGE overexpression induced cell cycle arrest at the G0-G1 phase in HaCaT cells (**Figure 5A**). However, treatment with Met at 100 μM for 48 h significantly corrected cell cycle arrest in HaCaT cells induced by RAGE

overexpression. Next, we measured p21, Gadd45a, CyclinB1, CyclinD1, and CDK4 protein levels in response to RAGE overexpression and Met treatment. After RAGE overexpression for 48 h, p21 and Gadd45a protein levels were significantly increased, and CyclinB1 and CDK4 protein levels were significantly decreased, respectively (**Figure 5B**). Treatment with Met at 100 μM for 48 h markedly corrected the cell cycle-related protein levels in HaCaT cells.

Met represses RAGE overexpression-induced cell apoptosis in HaCaT cells

To elucidate whether the cytoprotection of Met was associated with anti-apoptosis in RAGE overexpression-induced HaCaT cells, cell apoptosis was measured by annexin-V FITC/PI staining and flow cytometry analysis. As shown in **Figure 6A**, RAGE overexpression in HaCaT cells led to an increase in apoptotic cells compared to HaCaT cells with blank vector infection (46.23±1.30% vs. 2.97±0.17%). However, the increased cell apoptosis induced by RAGE overexpression was significantly inhibited by treatment with Met at 100 μM for 48 h in HaCaT cells. During the apoptotic process, mitochondrial membrane pores are opened and Δψmis disrupted. To assess the effect of RAGE overexpression and Met treatment on the changes in Δψm and ROS production in HaCaT cells, flow cytometry analysis was carried out to detect the fluorescence intensity of TMRE and DHE. As shown in **Figure 6B**, RAGE overexpression in HaCaT cells led to decreased Δψm (8933.36± 29.16 vs. 78467.59±27.76) and increased ROS production (59148.18±38.79 vs. 8550.22± 32.40) compared to HaCaT cells with blank vector infection, while treatment with Met at 100 μM for 48 h corrected Δψm and ROS production induced by RAGE overexpression (**Figure 6B** and **6C**). Next, we measured p53, caspase-3, Bax, and Bcl-2 protein levels in response to RAGE overexpression and Met treatment. After RAGE overexpression for 48 h, caspase-3 protein levels and the ratio of p-p53/p53 and Bax/Bcl-2 were significantly increased (**Figure 6D**). Treatment with Met at 100 μM markedly corrected the cell apoptosis-related protein levels in HaCaT cells.

Met represses RAGE overexpression-induced inflammatory factor secretions and activation of p38/NF-κB from HaCaT cells

Next, we measured TNF-α, IL-1β, IL-6, ICAM-1, and COX-2 secretions in response to RAGE overexpression and Met treatment. After RAGE overexpression, TNF-α, IL-1β, IL-6, ICAM-1, and COX-2 secretions were significantly increased, respectively, measured by ELISA assay (**Figure 7A-E**). Treatment with Met at 100 μM for 48 h markedly inhibited TNF-α, IL-1β, IL-6, ICAM-1, and COX-2 secretions from HaCaT cells. The protein levels of these inflammatory factors were also examined by western blotting as shown in **Figure 7F**. RAGE overexpression in HaCaT cells led to increases in the ratios of p-p38/p38 and p-NF-κBp65/NF-κBp65 compared with HaCaT cells with blank vector infection, while treatment with Met at 100 μM corrected activation of p38 and NF-κB induced by RAGE overexpression (**Figure 7G**). These findings suggest that Met possesses an anti-inflammatory effect and inactivation of p38/NF-κB in RAGE overexpression-induced HaCaT cells.

Discussion

Continual proliferation and differentiation of epidermal cells are normal processes required to maintain the structure and physiological function of healthy skin. Dysfunctions of these processes result in thinning skin, which is a common clinical outcome in diabetic patients [16]. In this study, a diabetic rat model, induced by STZ injection, was first established to prove the association between thin skin and diabetes, and then HaCaT cells were used as an *in vitro* model of keratinocytes. We observed a significant increase in the expression of RAGE in epidermal keratinocytes isolated from STZ-induced diabetic rats, in which RAGE ligand accumulation suggests an involvement of RAGE in diabetes-induced skin lesions. Previous general and histological observations have shown a diminution of the multilayer structure of keratinocytes in diabetic rats, implying that a dysfunction of keratinocyte proliferation may exist in diabetic skin [17]. In diabetes, RAGE expression is increased at sites of macrovascular and microvascular injury, as evidenced by its colocalization in susceptible organs including the heart, glomerulus, and retina [18-20].

To evaluate the role of RAGE in skin lesions, a stably expressing RAGE lentiviral vector was generated and infected into the HaCaT cells. Overexpression of RAGE in HaCaT cells showed a similar effect to STZ on induction of diabetes

in vivo, which inhibits cell proliferation and induction of cell cycle arrest and apoptosis. This is in agreement with our reported finding that the cell cycle of epidermal cells contains a markedly lower number of cells in the G2-M phase in diabetic rats compared with the control group [17]. Additionally, other factors involved in cell cycle progression and apoptosis were evaluated in this study. Our results showed that RAGE overexpression significantly increased expression of p21 and Gadd45a, while it decreased CyclinB1, CyclinD1, and CDK4 protein levels in HaCaT cells. Similarly, increased expression of apoptosis factors, including p38, caspase-3 and Bax/Bcl-2 ratio, was also found in HaCaT cells with RAGE overexpression.

Metformin (Met) is an important therapeutic agent in diabetic patients [21] and is widely used because of its effect on cancer proliferation [22]. Met can reduce cell proliferation of keratinocytes and block cell cycles which are associated with diminished activation or production of CyclinD1 and CDK4 [23], but it does not induce apoptosis [13]. However, Met treatment in HaCaT cells corrected inhibitory cell proliferation and G0-G1 cell cycle arrest as well as apoptosis induced by RAGE overexpression. These phenomena may be due to the different time points and concentrations of Met used, as well as the different cellular situations observed in this study. Furthermore, levels of key inflammatory factors, TNF-α, IL-1β, IL-6, ICAM-1, and COX-2, were significantly increased in RAGE-activated HaCaT cells, and reduced by treatment with soluble RAGE as reported in a previous study [24]. This is consistent with our finding that Met treatment corrected the increased secretion of these proinflammatory factors.

Met has therapeutic potential in diabetic nephropathy not only by inhibiting AGEs formation, but also by attenuating the deleterious effects of AGEs via down-regulating RAGE expression and subsequently suppressing ROS generation [11]. RAGE activated diverse signaling transduction cascades, leading to downstream consequences including ROS generation and activation of NF-κB followed by the release of proinflammatory factors and expression of growth factors associated with diabetic complications [25]. Moreover, p38MAPK, one of the most extensively studied cellular signaling cascades, plays a critical role in inflammation as it regulates the activation of NF-κB and induction of COX-2 in response to various external stimuli [26]. In the present study, RAGE overexpression promoted ROS generation and activation of p38 and NF-κB signaling, which was corrected by Met treatment in HaCaT cells. Administration of RAGE replicates the effects of hyperglycemia, whereas introduction of a RAGE antagonist completely or partially suppressed NF-κB activation and IL-6 transcripts [27, 28].

In conclusion, the biochemical and molecular findings of the present study reveal the anti-apoptosis and anti-inflammatory properties of Met against diabetic skin lesions. Inactivation of RAGE by Met provides a molecular basis for the anti-diabetic potential of Met.

Acknowledgements

This work was supported by the National Natural Science Foundation of China (81100585 and 81300672) and Shanghai Municipal Science and Technology Commission (No. 16431900502).

Disclosure of conflict of interest

None.

Address correspondence to: Dr. Jun-Jie Zou, Department of Endocrinology, Changzheng Hospital, Second Military Medical University, 415 Fengyang Road, Huangpu District, Shanghai 200003, China. Tel: +86-21-81885375; Fax: +86-21-63586228; E-mail: zjj1688@163.com; Dr. Wan-Qing Liao, Department of Dermatology, Changzheng Hospital, Second Military Medical University, 415 Fengyang Road, Huangpu District, Shanghai 200003, China. Tel: +86-21-81885375; Fax: +86-21-63586228; E-mail: liaowanqing@sohu.com

References

[1] Park J, Peters PA. Mortality from diabetes mellitus, 2004 to 2008: A multiple-cause-of-death analysis. Health Rep 2014; 25: 12-6.

[2] Guariguata L, Whiting D, Hambleton I, Beagley J, Linnenkamp U, Shaw J. Global estimates of diabetes prevalence for 2013 and projections for 2035. Diabetes Res Clin Pract 2014; 103: 137-149.

[3] Wondrak GT, Roberts MJ, Jacobson MK, Jacobson EL. Photosensitized growth inhibition

of cultured human skin cells: mechanism and suppression of oxidative stress from solar irradiation of glycated proteins. J Invest Dermatol 2002; 119: 489-498.
[4] Wendt T, Harja E, Bucciarelli L, Qu W, Lu Y, Rong LL, Jenkins DG, Stein G, Schmidt AM, Yan SF. RAGE modulates vascular inflammation and atherosclerosis in a murine model of type 2 diabetes. Atherosclerosis 2006; 185: 70-77.
[5] Jensen LJ, Denner L, Schrijvers BF, Tilton RG, Rasch R, Flyvbjerg A. Renal effects of a neutralising RAGE-antibody in long-term streptozotocin-diabetic mice. J Endocrinol 2006; 188: 493-501.
[6] Ramasamy R, Vannucci SJ, Du Yan SS, Herold K, Yan SF, Schmidt AM. Advanced glycation end products and RAGE: a common thread in aging, diabetes, neurodegeneration, and inflammation. Glycobiology 2005; 15: 16R-28R.
[7] Chang JS, Wendt T, Qu W, Kong L, Zou YS, Schmidt AM, Yan SF. Oxygen deprivation triggers upregulation of early growth response-1 by the receptor for advanced glycation end products. Circ Res 2008; 102: 905-913.
[8] Kim JY, Park HK, Yoon JS, Kim SJ, Kim ES, Ahn KS, Kim DS, Yoon SS, Kim BK, Lee YY. Advanced glycation end product (AGE)-induced proliferation of HEL cells via receptor for AGE-related signal pathways. Int J Oncol 2008; 33: 493-501.
[9] Liu Y, Yang F, Ma W, Sun Q. Metformin inhibits proliferation and proinflammatory cytokines of human keratinocytes in vitro via mTOR-signaling pathway. Pharm Biol 2016; 54: 1173-8.
[10] Li W, Ma W, Zhong H, Liu W, Sun Q. Metformin inhibits proliferation of human keratinocytes through a mechanism associated with activation of the MAPK signaling pathway. Exp Ther Med 2014; 7: 389-392.
[11] Ishibashi Y, Matsui T, Takeuchi M, Yamagishi SI. Beneficial effects of metformin and irbesartan on advanced glycation end products (AGEs)-RAGE-induced proximal tubular cell injury. Pharmacol Res 2012; 65: 297-302.
[12] Ishibashi Y, Matsui T, Takeuchi M, Yamagishi S. Metformin inhibits advanced glycation end products (AGEs)-induced renal tubular cell injury by suppressing reactive oxygen species generation via reducing receptor for AGEs (RAGE) expression. Horm Metab Res 2012; 44: 891-895.
[13] Ochoa-Gonzalez F, Cervantes-Villagrana AR, Fernandez-Ruiz JC, Nava-Ramirez HS, Hernandez-Correa AC, Enciso-Moreno JA, Castañeda-Delgado JE. Metformin induces cell cycle arrest, reduced proliferation, wound healing impairment in vivo and is associated to clinical outcomes in diabetic foot ulcer patients. PLoS One 2016; 11: e0150900.
[14] Zhu Z, Hotchkiss SA, Boobis AR, Edwards RJ. Expression of P450 enzymes in rat whole skin and cultured epidermal keratinocytes. Biochem Biophys Res Commun 2002; 297: 65-70.
[15] Yuan Y, Zhang J, Cai L, Ding C, Wang X, Chen H, Wang X, Yan J, Lu J. Leptin induces cell proliferation and reduces cell apoptosis by activating c-myc in cervical cancer. Oncol Rep 2013; 29: 2291-2296.
[16] Wang CM, Lincoln J, Cook JE, Becker DL. Abnormal connexin expression underlies delayed wound healing in diabetic skin. Diabetes 2007; 56: 2809-2817.
[17] Chen XF, Lin WD, Lu SL, Xie T, Ge K, Shi YQ, Zou JJ, Liu ZM, Liao WQ. Mechanistic study of endogenous skin lesions in diabetic rats. Exp Dermatol 2010; 19: 1088-1095.
[18] Candido R, Forbes JM, Thomas MC, Thallas V, Dean RG, Burns WC, Tikellis C, Ritchie RH, Twigg SM, Cooper ME, Burrell LM. A breaker of advanced glycation end products attenuates diabetes-induced myocardial structural changes. Circ Res 2003; 92: 785-792.
[19] Doublier S, Salvidio G, Lupia E, Ruotsalainen V, Verzola D, Deferrari G, Camussi G. Nephrin expression is reduced in human diabetic nephropathy evidence for a distinct role for glycated albumin and angiotensin II. Diabetes 2003; 52: 1023-1030.
[20] Zong H, Ward M, Madden A, Yong PH, Limb GA, Curtis TM, Stitt AW. Hyperglycaemia-induced pro-inflammatory responses by retinal Müller glia are regulated by the receptor for advanced glycation end-products (RAGE). Diabetologia 2010; 53: 2656-2666.
[21] Noto H, Goto A, Tsujimoto T, Noda M. Cancer risk in diabetic patients treated with metformin: a systematic review and meta-analysis. PLoS One 2012; 7: e33411.
[22] Schuler KM, Rambally BS, DiFurio MJ, Sampey BP, Gehrig PA, Makowski L, Bae-Jump VL. Antiproliferative and metabolic effects of metformin in a preoperative window clinical trial for endometrial cancer. Cancer Med 2015; 4: 161-173.
[23] Quattrini I, Conti A, Pazzaglia L, Novello C, Ferrari S, Picci P, Benassi MS. Metformin inhibits growth and sensitizes osteosarcoma cell lines to cisplatin through cell cycle modulation. Oncol Rep 2014; 31: 370-375.
[24] Chen Y, Yan SS, Colgan J, Zhang HP, Luban J, Schmidt AM, Stern D, Herold KC. Blockade of late stages of autoimmune diabetes by inhibition of the receptor for advanced glycation end products. J Immunol 2004; 173: 1399-1405.
[25] Bierhaus A, Humpert PM, Morcos M, Wendt T, Chavakis T, Arnold B, Stern DM, Nawroth PP. Understanding RAGE, the receptor for ad-

vanced glycation end products. J Mol Med (Berl) 2005; 83: 876-886.
[26] Kyriakis JM, Avruch J. Mammalian mitogen-activated protein kinase signal transduction pathways activated by stress and inflammation. Physiol Rev 2001; 81: 807-869.
[27] Okamoto K, Martin DP, Schmelzer JD, Mitsui Y, Low PA. Pro-and anti-inflammatory cytokine gene expression in rat sciatic nerve chronic constriction injury model of neuropathic pain. Exp Neurol 2001; 169: 386-391.
[28] Bierhaus A, Haslbeck KM, Humpert PM, Liliensiek B, Dehmer T, Morcos M, Sayed AA, Andrassy M, Schiekofer S, Schneider JG, Schulz JB, Heuss D, Neundörfer B, Dierl S, Huber J, Tritschler H, Schmidt AM, Schwaninger M, Haering HU, Schleicher E, Kasper M, Stern DM, Arnold B, Nawroth PP. Loss of pain perception in diabetes is dependent on a receptor of the immunoglobulin superfamily. J Clin Invest 2004; 114: 1741-1751.